ATOMIZED SPRAY PLASMA DEPOSITION OF STRUCTURALLY WELL-DEFINED BIOACTIVE COATINGS

T. J. Wood, P. S. Brown, and J. P. S. Badyal*

Department of Chemistry,
Science Laboratories,
Durham University,
Durham DH1 3LE
England, UK

* Corresponding author email: j.p.badyal@durham.ac.uk

TABLE OF CONTENTS GRAPHIC

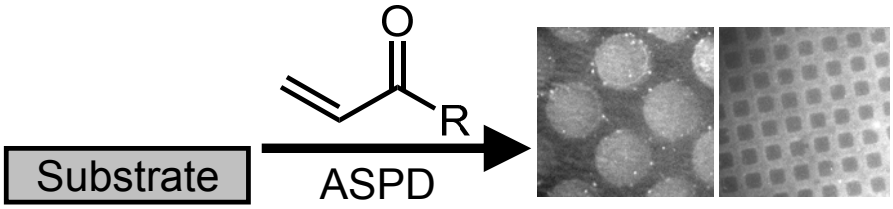

ABSTRACT

Structurally well-defined bioactive films have been prepared in a single solventless step by atomizing precursor molecules into a non-equilibrium electrical discharge. By way of example, atomized spray plasma deposition (ASPD) is used to form poly(alkyl acrylate) arrays for phospholipid immobilization, and poly(*N*-acryloylsarcosine methyl ester) protein-resistant surfaces.

Keywords: Atomized spray plasma deposition; plasma polymer; phospholipid; lipophilic; protein resistance.

1. INTRODUCTION

Bioactive surfaces are important for a plethora of applications including biocompatible implants,[1,2] the study of biological processes,[3] and the prevention of biofouling.[4] For instance, immobilized phospholipid surfaces[5] are used for biosensing,[6,7] biomimesis,[8,9] bioseparation,[10] vesicle binding,[11,12] biocompatibility,[13,14] and enzyme immobilization.[15] Phospholipids are a type of amphiphilic lipid comprising a hydrophilic phosphate head group and a straight alkyl chain hydrophobic tail group. They play an important structural role in the cell membrane through hydrophobic interactions between tail groups to form a lipid bilayer.[16] Previously, phospholipid surfaces have been prepared using graft polymerization,[17,18] self-assembled monolayers of alkanethiols,[19,20,21] thiolipids,[22] or silanes[23,24] (to form lipid bilayers). Another noteworthy class of bioactive surfaces is protein-resistant coatings which are highly sought after for antifouling applications[25] and cell-resistant biomedical devices.[26] Some examples include poly(ethylene glycol),[27,28,29] polyacrylamide,[30] or polysaccharide[31,32,33] layers formed by physisorption,[34] graft polymerization,[35,36] plasmachemical deposition,[37,38,39] or self-assembled monolayers (SAMs).[27,40,41] Many of these preparative methods for bioactive surfaces tend to suffer from inherent limitations: physisorption is by its very nature reversible; graft polymerization requires an initiator layer[42] or surface functionalisation prior to commencing the grafting step;[17,35] whilst self-assembled monolayers are substrate-specific[43,44] and can be moisture sensitive (e.g. silanes[45]) or unstable in oxidative chemical environments (e.g. thiols[46]).

In contrast to the aforementioned drawbacks, plasmachemical deposition is a solventless, substrate-independent method for thin film production.[47] In the past it has been shown that structurally well-defined functional nanocoatings can be prepared by pulsed plasmachemical deposition, which involves modulating an electrical discharge in the presence of precursor vapour on the microsecond-millisecond timescale.[48] In order to achieve higher deposition rates, it becomes necessary to increase the pressure or flow rate of the precursor vapour, thereby lowering the average plasma input energy per precursor molecule[47,49]; however this ultimately leads to plasma instabilities and eventual electrical discharge extinction. Furthermore, solid precursors cannot be utilized due to their lack of sufficient vapour pressure. These shortcomings can be circumvented by utilising an atomized spray

of the precursor molecule to provide localized high concentrations of monomer in the form of fine droplets which are effectively less perturbing to the overall collective plasma stability phenomena (compared to the far greater pressures for equivalent vapour phase precursor concentrations).[50,51,52] In addition, low vapour pressure solid precursors can be utilized by mixing with liquid precursors to facilitate direct atomization into the plasma excitation medium.

In this article, we report on the atomized spray plasma deposition (ASPD) of poly(alkyl acrylate) layers in order to explore the influence of alkyl chain length upon surface lipophilicity, and poly(*N*-acryloylsarcosine methyl ester) films for protein resistance, Scheme 1.

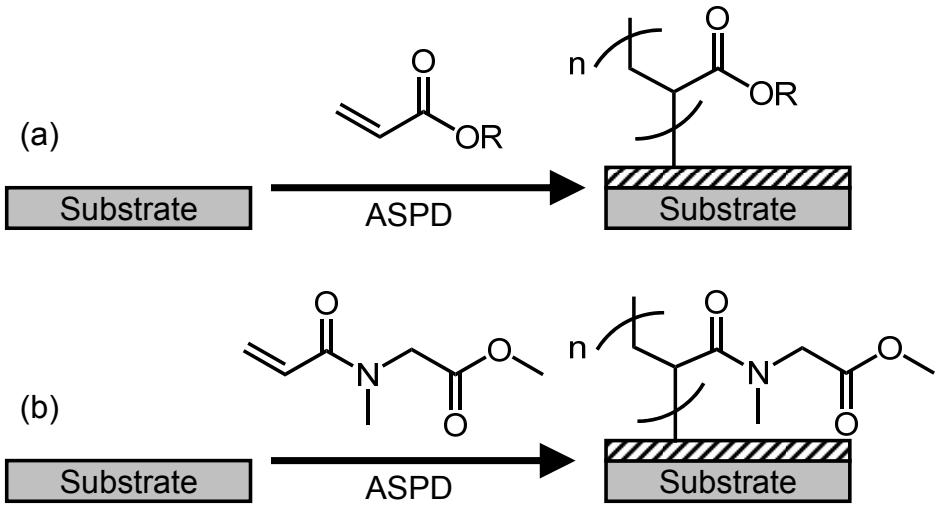

Scheme 1: Atomized spray plasma deposition (ASPD) of: (a) lipophilic poly(alkyl acrylate) layers (R = C_6H_{13}, $C_{12}H_{25}$, $C_{18}H_{37}$); and (b) protein-resistant poly(*N*-acryloylsarcosine methyl ester) layers.

2. EXPERIMENTAL

2.1 Atomized Spray Plasma Deposition

Plasmachemical deposition was carried out in an electrodeless cylindrical glass T-shape reactor (volume 820 cm^3, base pressure of 3 x 10^{-3} mbar, and with a leak rate better than 2 x 10^{-9} mol s^{-1}), enclosed in a Faraday cage. The atomized spray precursor inlet was surrounded by a copper coil (4 mm diameter, 7 turns), Figure 1.

The chamber was pumped down using a 30 L min^{-1} rotary pump attached to a liquid nitrogen cold trap, and a Pirani gauge was used to monitor system pressure. The output impedance of a 13.56 MHz radio frequency (rf) power supply was matched to the partially ionized gas load via an inductor-capacitor (L-C) matching unit connected to the copper coil. Prior to each deposition, the reactor was scrubbed using detergent, rinsed with propan-2-ol, and dried in an oven. A continuous wave air plasma was then run at 0.2 mbar pressure and 50 W power for 30 min in order to remove any remaining trace contaminants from the chamber walls. Substrates used for coating were pieces of silicon (100) wafer (Silicon Valley Microelectronics Inc.), PTFE (Goodfellow Cambridge Ltd.), and polypropylene (Lawson-Mardon Ltd., capacitor grade); these were placed downstream from the atomizer nozzle. Precursors used for atomized spray plasma deposition were *n*-hexyl acrylate (liquid, +98%, Sigma-Aldrich Ltd.), *n*-dodecyl acrylate (liquid, +90% Sigma-Aldrich Ltd.), *n*-octadecyl acrylate (solid, +97%, Sigma-Aldrich Ltd., dissolved to form a 1:3 mixture with *n*-dodecyl acrylate), and *N*-acryloylsarcosine methyl ester (+97%, Alfa Aesar Ltd.). Each precursor was loaded into a sealable glass tube, degassed using several freeze-pump-thaw cycles, and then was introduced into the reactor at a flow rate of 0.02 mL s^{-1} (mediated by a needle metering valve) via an ultrasonic nozzle (Model No. 8700-120, Sono Tek Corp.) operating at 120 kHz. Deposition entailed running a 50 W continuous wave plasma for 150 s whilst concurrently atomizing the precursor. Upon plasma extinction, the system was evacuated to base pressure, and then vented to atmosphere. The films were well adhered and stable towards polar and non-polar solvent washing. Control experiments showed that in the absence of plasma excitation, the deposited layers could be easily washed off with solvent. Typically, a minimum of 3-5 samples were analysed.

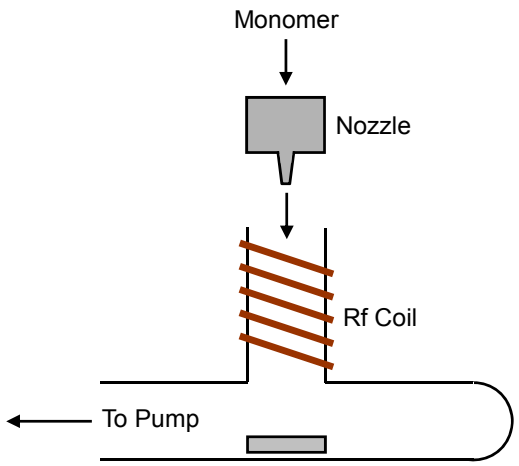

Figure 1: Atomized spray plasma deposition chamber.

2.2 Film Characterization

Surface elemental compositions were determined by X-ray photoelectron spectroscopy (XPS) using a VG ESCALAB II electron spectrometer equipped with a non-monochromated Mg Kα X-ray source (1253.6 eV) and a concentric hemispherical analyser. Photoemitted electrons were collected at a take-off angle of 20° from the substrate normal, with electron detection in the constant analyser energy mode (CAE, pass energy = 20 eV). Experimentally determined instrument sensitivity (multiplication) factors were taken as C(1s):O(1s):N(1s) equals 1.00:0.36:0.63. All binding energies were referenced to the C(1s) hydrocarbon peak at 285.0 eV. A linear background was subtracted from core level spectra and then fitted to Gaussian peak shapes with a constant full-width-half-maximum (fwhm).[53,54]

Infrared spectra were acquired using a FTIR spectrometer (Perkin-Elmer Spectrum One) fitted with a liquid nitrogen cooled mercury cadmium telluride (MCT) detector operating at 4 cm^{-1} resolution across the 700–4000 cm^{-1} range. Attenuated-total-reflection spectra were obtained using a Golden Gate accessory (Specac Ltd.).

Sessile drop water contact angle measurements were performed at ambient temperature using a video capture apparatus (VCA2500XE, A.S.T. Products Inc.) in combination with a motorized syringe dispensing a 1 μL droplet size. High purity water (B.S. 3978 grade 1) was used as the probe liquid.

Film thicknesses were measured using a spectrophotometer (nkd-6000, Aquila Instruments Ltd.). Transmittance-reflectance curves (350–1000 nm

wavelength range) were acquired for each deposited layer and fitted to a Cauchy material model using a modified Levenberg-Marquardt algorithm.[55]

2.3 Bioactivity Testing

In the case of the alkyl acrylates, atomized spray plasma deposition was performed through a 100 mesh brass grid (pitch 250 μm, hole width 205 μm, bar width 45 μm) onto PTFE pieces in order to produce bioarrays, which were then tested for bioactivity by sequential immersion into solutions of 20 μg mL^{-1} phospholipid-biotin conjugate (KODE Biotech Ltd.) followed by 20 μg mL^{-1} avidin-FITC conjugate (Invitrogen Corp.) in phosphate buffered saline solution (Invitrogen Corp.), where FITC is a fluorescent tag. Between each immersion, the substrate was thoroughly rinsed with deionized water and washed in phosphate buffered saline solution in order to remove any non-bound surface species.

For *N*-acryloylsarcosine methyl ester, atomized spray plasma deposition was carried out through a 1500 mesh nickel grid (pitch 16.5 μm, hole width 11.5 μm, bar width 5 μm) onto polypropylene pieces, and these were then immersed into a 50 μg mL^{-1} Protein A–FITC conjugate (Sigma-Aldrich Ltd.) in phosphate buffered saline solution, and subsequently rinsed with deionized water and washed in phosphate buffered saline solution to remove any non-bound surface species.

Fluorescence microscopy was performed using an Olympus IX-70 system (DeltaVision RT, Applied Precision Inc.). Images were collected using excitation wavelengths at 490±25 nm and emission wavelengths at 528±40 nm corresponding to the absorption/emission maxima of 494/518 nm for the FITC fluorescent tag.

3. RESULTS

3.1 Atomized Spray Plasma Deposition of Lipophilic Poly(Alkyl Acrylate) Layers

The absence of any Si(2p) XPS signal from the underlying silicon substrate confirmed that complete surface coverage had been achieved by atomized spray plasma deposition, Table 1. For the atomized spray plasma deposited poly(alkyl acrylate) layers, there is good agreement between the measured carbon-to-oxygen elemental ratios and those expected theoretically (with just a slight reduction in

oxygen). Angle-resolved XPS analysis revealed no significant change in these ratios, which indicates no surface ordering of the alkyl chains. There are three distinctive components in the C(1s) XPS spectrum corresponding to hydrocarbon ($\underline{C}_xH_y$) at 285.0 eV, as well as oxygenated carbon centres, $\underline{C}$-O (at 286.6 eV), and O-$\underline{C}$=O (at 288.9 eV), Figure 2. The decrease in intensity of the oxygenated carbon component peaks with increasing alkyl chain length for the poly(alkyl acrylate)s is consistent with the theoretically predicted trend, Table 1. In the case of the atomized spray deposited poly(dodecyl acrylate-*co*-octadecyl acrylate) layers, the films most likely contain a random arrangement of the respective monomers.

Table 1: Elemental XPS percentages for atomized spray plasma deposited layers.

Functional Film	**XPS Elemental Ratios**		
	%C	**%O**	**%N**
Theoretical poly(hexyl acrylate)	81.8	18.2	—
ASPD poly(hexyl acrylate)	84±1	16 ±1	—
Theoretical poly(dodecyl acrylate)	88.2	11.8	—
ASPD poly(dodecyl acrylate)	90±1	10±1	—
Theoretical poly(dodecyl acrylate-*co*-octadecyl acrylate)	89.3	10.7	—
ASPD poly(dodecyl acrylate-*co*-octadecyl acrylate)	92±1	8±1	—
Theoretical poly(*N*-acryloylsarcosine methyl ester)	63.6	27.3	9.1
ASPD poly(*N*-acryloylsarcosine methyl ester)	69±3	20±2	11±2

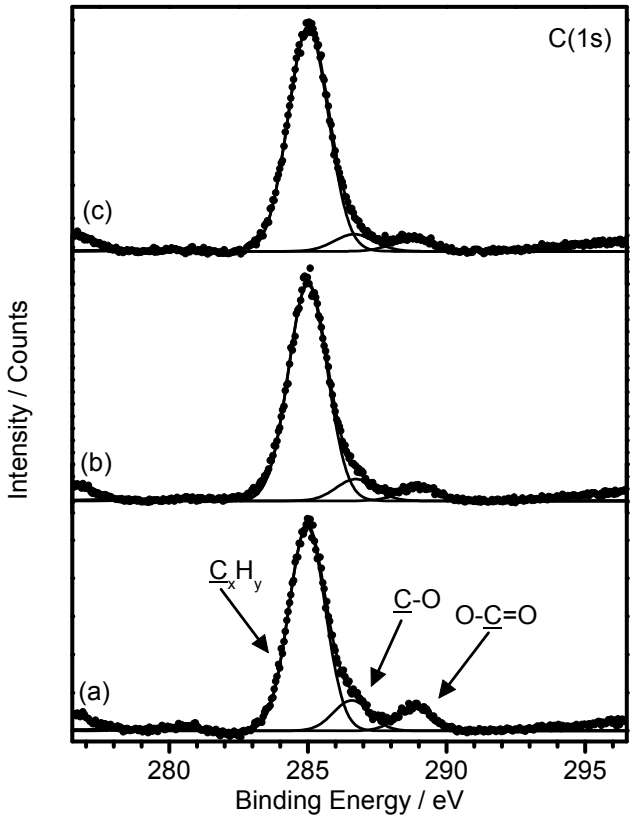

Figure 2: C(1s) X-ray photoelectron spectra of atomized spray plasma deposited: (a) poly(hexyl acrylate); (b) poly(dodecyl acrylate); and (c) poly(dodecyl acrylate-*co*-octadecyl acrylate).

Infrared spectroscopy provided additional evidence of high levels of structural retention for the atomized spray plasma deposited poly(alkyl acrylate) layers, Table 2 and Figure 3. Alkyl C-H and carbonyl C=O stretch vibrations are retained; whilst there is a disappearance of absorbances associated with the C=C acrylate bond, which is indicative of conventional carbon-carbon double bond polymerization taking place during ASPD. For each poly(alkyl acrylate) layer the carbonyl C=O stretch shifts to higher wavenumbers by 10–18 cm^{-1} compared to its monomer, which is consistent with a change in chemical environment from a conjugated carbonyl group (i.e. an acrylate) to an unconjugated carbonyl group (i.e. polymerization).[56]

Table 2: Infrared absorbances of alkyl acrylate precursors and the corresponding atomized spray plasma deposited polymer layers.

Assignment	**FTIR Absorbance / cm^{-1}**					
	Hexyl acrylate		**Dodecyl acrylate**		**Octadecyl acrylate**	**APSD Dodecyl acrylate-*co*-Octadecyl acrylate**
	Precursor	ASPD	Precursor	ASPD		
$\nu_{as}(CH_3)$	2956	2958	2955	2954	2952	2953
$\nu_{as}(CH_2)$	2930	2932	2922	2922	2917	2920
$\nu_{s}(CH_3)$	2872	2872	2871	2871	2869	2871
$\nu_{s}(CH_2)$	2860	2860	2853	2853	2848	2852
ν(C=O)	1723	1741	1725	1735	1720	1730
ν(C=C)	1637 1620	—	1637 1620	—	1633	—
=CH wag	984	—	983	—	976	—
$=CH_2$ wag	963	—	962	—	963	—
$=CH_2$ twist	809	—	809	—	814	—

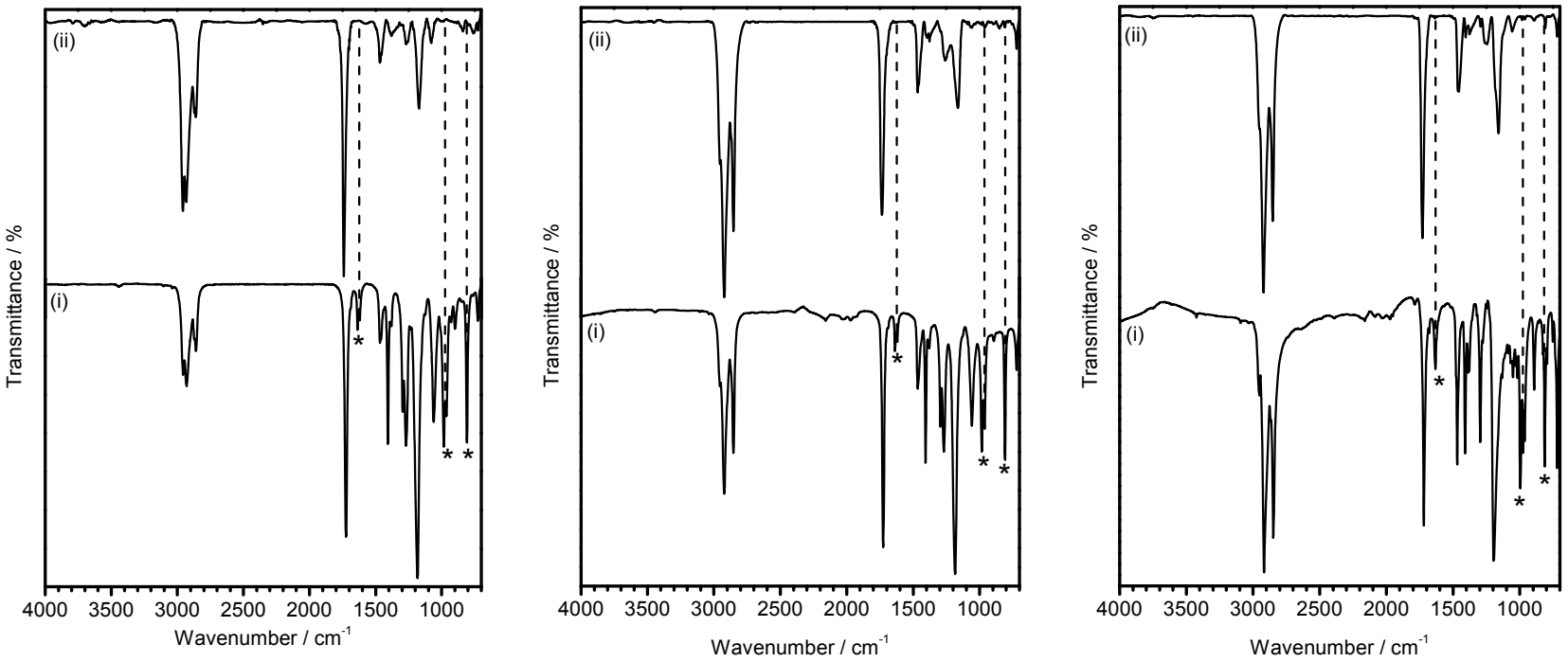

Figure 3: Infrared spectra of: (i) monomer; and (ii) atomized spray plasma deposited layer for (a) hexyl acrylate; (b) dodecyl acrylate; and (c) octadecyl acrylate monomer with poly(dodecyl acrylate-*co*-octadecyl acrylate) as the deposited layer. * Denotes polymerizable C=C double bond stretches.

Contact angle analysis showed that the atomized spray plasma deposited poly(alkyl acrylate) layers all exhibit static water contact angles of 80°, which is consistent with the hydrophobic nature of the polymer alkyl chain side group, [57] Table 3.

The measured film growth rates were found to be significantly greater for all of the atomized spray plasma deposited films compared to previously reported vapour phase techniques (by at least a factor of 20),[58] Table 3. The deposition rate was found to decrease with increasing alkyl chain length, which correlates to a lower concentration of acrylate polymerization groups (given the corresponding increase in molecular mass of the precursor and constant delivery flow rate).

Table 3: Equilibrium water contact angles and atomized spray plasma deposition rates.

Atomized Spray Plasma Deposited Layer	**Equilibrium Water Contact Angle / °**	**Deposition Rate / nm min^{-1}**
Poly(hexyl acrylate)	80±1	4500±300
Poly(dodecyl acrylate)	80±1	3500±200
Poly(dodecyl acrylate-*co*-octadecyl acrylate)	80±1	3100±200
Poly(*N*-acryloylsarcosine methyl ester)	53±1	195±9

Fluorescence micrographs of atomized spray plasma deposited poly(hexyl acrylate) and poly(dodecyl acrylate) films exposed to phospholipid-biotin and then avidin-FITC solutions displayed negligible fluorescence, Figures 4 and 5. In contrast, the poly(dodecyl acrylate-*co*-octadecyl acrylate) layer containing the longer $C_{18}H_{37}$ alkyl chain showed significant phospholipid binding indicative of stronger hydrophobic interactions between the alkyl chain side groups and the phospholipid, which can be attributed to the interdigitation of the 18-membered phosholipid alkyl groups with the 18-membered alkyl chains present in the octadecyl acrylate moiety (this is in contrast to phospholipid bilayer formation on alkyl-containing self-assembled monolayers, where lipid binding is independent of alkyl chain length[20]). As a control experiment, no fluorescence signal was detected following exposure of

the poly(dodecyl acrylate-*co*-octadecyl acrylate) layer to just the avidin–FITC conjugate solution.

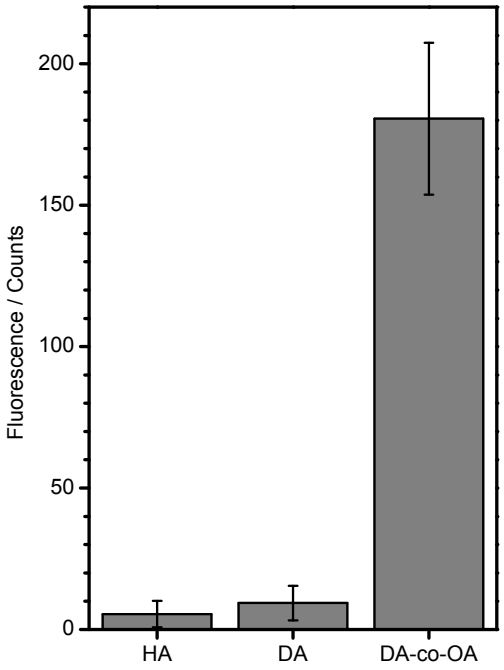

Figure 4: Fluorescence intensity for atomized spray plasma deposited layers exposed to phospoholipid-biotin and then avidin-FITC solutions (HA = poly(hexyl acrylate), DA = poly(dodecyl acrylate), and DA-co-OA = poly(dodecyl acrylate-*co*-octadecyl acrylate).

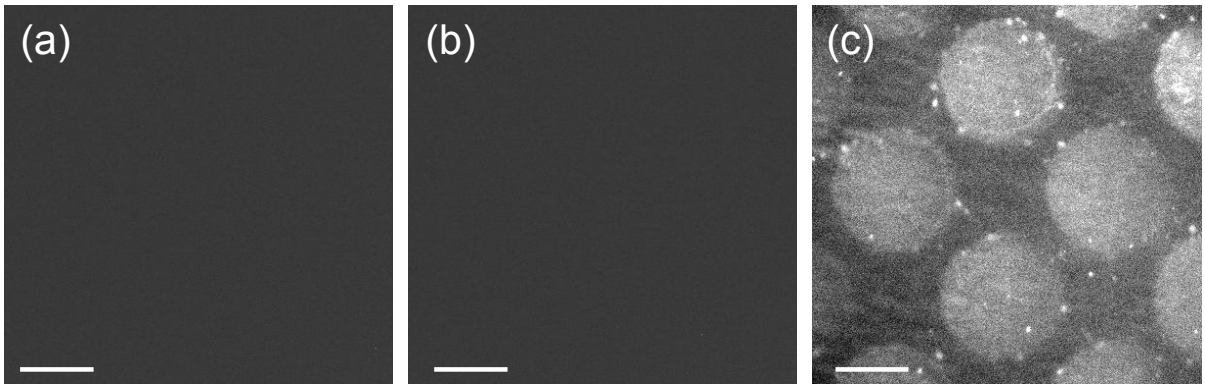

Figure 5: Fluorescence micrographs of atomized spray plasma deposited arrays exposed to phospholipid-biotin and then avidin-FITC solutions: (a) poly(hexyl acrylate); (b) poly(dodecyl acrylate); and (c) poly(dodecyl acrylate-*co*-octadecyl acrylate). White scale bar = 100 μm.

3.2 Atomized Spray Plasma Deposition of Protein-Resistant Poly(N-Acryloylsarcosine Methyl Ester) Layers

XPS analysis of the atomized spray plasma deposited poly(*N*-acryloylsarcosine methyl ester) layers showed reasonable agreement between the theoretical and experimental elemental concentrations, Table 1. The XPS C(1s) spectrum can be fitted to the following components:[39] $\underline{C}_xH_y/\underline{C}$-N (285.0 eV), N-$\underline{C}$-COO (285.7 eV), $\underline{C}$-O/N-$\underline{C}$=O (286.7 eV), and O-$\underline{C}$=O (288.6 eV), Figure 6.

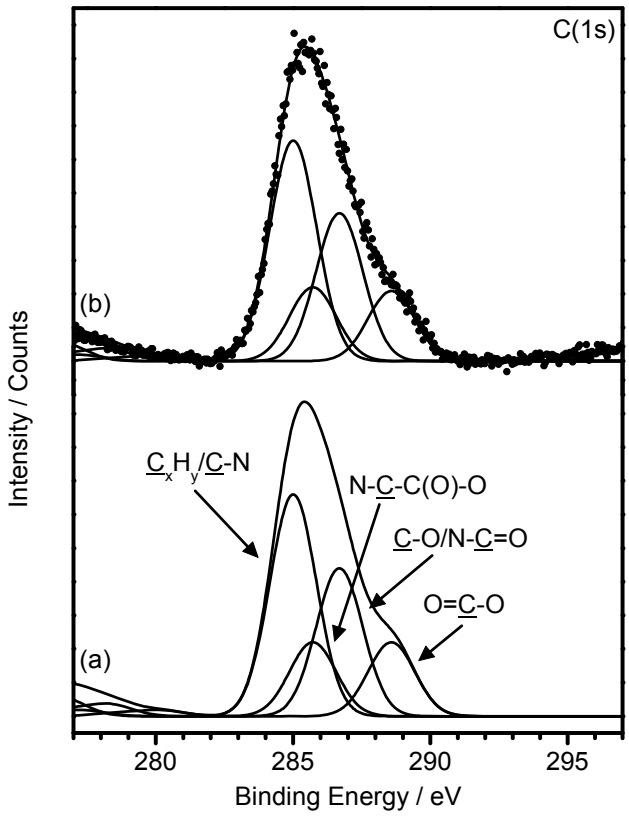

Figure 6: X-ray photoelectron specta of: (a) theoretical poly(*N*-acryloylsarcosine methyl ester); and (b) atomized spray plasma deposited poly(*N*-acryloylsarcosine methyl ester).

The following infrared bands can be assigned to the *N*-acryloylsarcosine methyl ester monomer: $\nu_{as}(CH_3)$ stretch (2954 cm^{-1}), ν(C=O) carbonyl ester stretch (1743 cm^{-1}), ν(C=O) carbonyl amide stretch (1649 cm^{-1}), ν(C=C) vinyl stretch (1612 cm^{-1}), the ν(C-O) ester stretch (1201 cm^{-1}), and the $=CH_2$ twist (795 cm^{-1}),[39,56] Figure 7. Infrared spectroscopy indicated good structural retention for the atomized spray

plasma deposited poly(*N*-acryloylsarcosine methyl ester) films. The absorbances associated with the carbon-carbon double bond are seen to have disappeared, which is consistent with conventional polymerization having taken place during atomized spray plasma deposition.

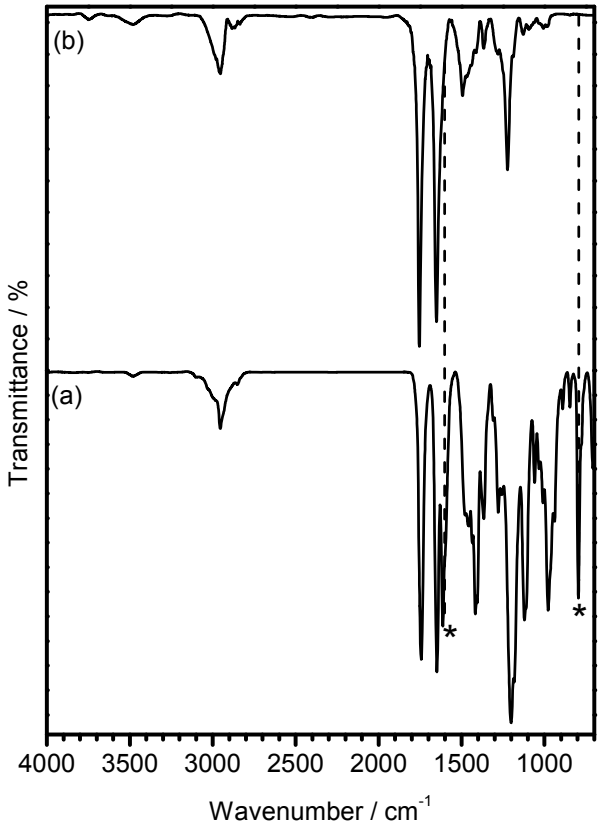

Figure 7: Infrared spectra of: (a) *N*-acryloylsarcosine methyl ester; and (b) atomized spray plasma deposited poly(*N*-acryloylsarcosine methyl ester). * Denotes polymerizable C=C double bond stretches.

The static water contact angle for atomized spray plasma deposited poly(*N*-acryloylsarcosine methyl ester) films is consistent with previous studies for poly(*N*-acryloylsarcosine methyl ester) layers,[59] Table 3. The observed hydrophilicity stems from the terminal ester group and the amide linkages within the polymer backbone.[39] A factor of 20 enhancement in deposition rate was measured compared to conventional vapour-phase approaches,[59] Table 3.

Fluorescence micrographs of atomized spray plasma deposited poly(*N*-acryloylsarcosine methyl ester) films through a grid and then exposed to Protein A–

FITC displayed negative images, which verified that these surfaces are protein resistant compared to the masked uncoated (protein binding) regions, Figure 8.

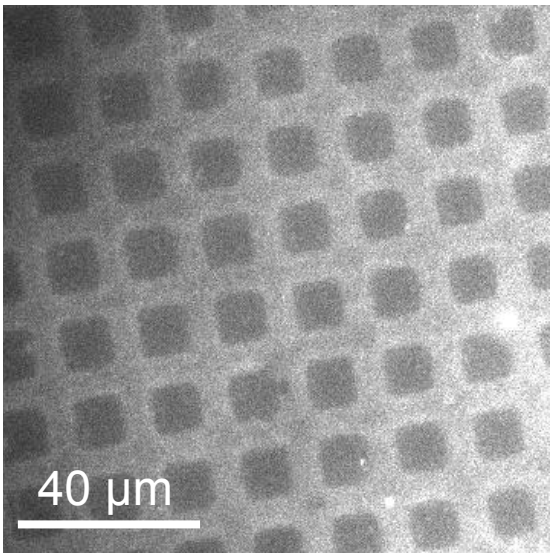

Figure 8: Fluorescence micrograph of poly(*N*-acryloylsarcosine methyl ester) films prepared by atomized spray plasma deposition through a grid and then exposed to Protein A–FITC solution.

4. DISCUSSION

Atomized spray plasma deposition provides a substrate-independent, solventless technique to yield functional coatings. Plasma excited species (VUV, electrons, ions) activate the substrate surface in conjunction with initiating polymerization at the carbon-carbon double bond contained in the precursor molecules (which are introduced into the plasma medium as a fine mist of small droplets — around 25 µm in size[60]). Polymer chain growth propagates within the droplets and during substrate impact culminating in rapid film growth. The measured deposition rates for the poly(alkyl acrylate) and poly(*N*-acryloylsarcosine methyl ester) bioactive coatings far exceed those reported for conventional vapour-phase deposition techniques,[58,59] Furthermore by utilization of an atomized spray, the negligible vapour pressures of dodecyl acrylate and octadecyl acrylate are no longer a limitation. Unlike previously reported atmospheric pressure atomized spray plasma deposition processes, the present approach circumvents the requirement for expensive diluent gases such as

helium,[50,51] and avoids plasma-induced damage of the growing film[61] by positioning of the substrate downstream from the atomizer nozzle. Such fast deposition rates combined with high levels of functionality (structural retention) makes this technique amenable to high-throughput manufacturing (such as roll-to-roll processing). Also, in contrast to electrospray ionization (ESI) and Atmospheric-Pressure Chemical Ionization (APCI) deposition techniques, this approach circumvents the requirement for preformed polymers, solvents, and conductive substrates.[62]

5. CONCLUSIONS

Lipophilic poly(alkyl acrylate) and protein-resistant poly(*N*-acryloylsarcosine methyl ester) bioactive coatings have been prepared in a single, solventless step using atomized spray plasma deposition (ASPD). Film growth rates are significantly enhanced compared to conventional techniques. Furthermore, low vapour pressure solid precursors can be utilized by mixing with liquid precursors to facilitate their direct atomization into the plasma medium.

6. ACKNOWLEDGMENTS

T. J. Wood would like to thank Surface Innovations Ltd. for financial support. The authors are grateful to KODE Biotech Ltd. (NZ) for providing a sample of the phospholipid-biotin conjugate.

7. REFERENCES

(1) Hench, L. L.; Wilson, J. Surface-Active Biomaterials. *Science* **1984**, *226*, 630–636.

(2) Meyers, S. R.; Grinstaff, M. W. Biocompatible and Bioactive Surface Modifications for Prolonged In Vivo Efficacy. *Chem. Rev.* **2012**, *112*, 1615–1632.

(3) Messersmith, P. B. Multitasking in Tissues and Materials. *Science* **2008**, *319*, 1767–1768.

(4) Statz, A. R.; Meagher, R. J.; Barron, A. E.; Messersmith, P. B. New Peptidomimetic Polymers for Antifouling Surfaces. *J. Am. Chem. Soc.* **2005**, *127*, 7972–7973.

(5) Sackmann, E. Supported Membranes: Scientific and Practical Applications. *Science* **1996**, *271*, 43–48.

(6) Cornell, B. A.; Braach-Maksvytis, V. L. B.; King, L. G.; Osman, P. D. J.; Raguse, B.; Wieczorek, L.; Pace, R. J. A Biosensor that Uses Ion-Channel Switches. *Nature* **1997**, *387*, 580–583.

(7) Stora, T.; Lakey, J. H.; Vogel, H. Ion-Channel Gating in Transmembrane Receptor Proteins: Functional Activity in Tethered Lipid Membranes. *Angew. Chem. Int. Ed.* **1999**, *38*, 389–392.

(8) Plant, A. L.; Gueguetchkeri, M.; Yap, W. Supported Phospholipid/Alkanethiol Biomimetic Membranes: Insulating Properties. *Biophys. J.* **1994**, *67*, 1126–1133.

(9) Naumann, C. A.; Prucker, O.; Lehmann, T.; Rühe, J.; Knoll, W.; Frank, C. W. The Polymer-Supported Phospholipid Bilayer: Tethering as a New Approach to Substrate−Membrane Stabilization. *Biomacromolecules* **2002**, *3*, 27–35.

(10) van Oudenaarden, A.; Boxer, S. G. Brownian Ratchets: Molecular Separations in Lipid Bilayers Supported on Patterned Arrays. *Science* **1999**, *285*, 1046–1048.

(11) Stanish, I.; Santos, J. P.; Singh, A. One-Step, Chemisorbed Immobilization of Highly Stable, Polydiacetylenic Phospholipid Vesicles onto Gold Films. *J. Am. Chem. Soc.* **2001**, *123*, 1008–1009.

(12) Zhang, L.; Hong, L.; Yu, Y.; Bae, S. C.; Granick, S. Nanoparticle-Assisted Surface Immobilization of Phospholipid Liposomes. *J. Am. Chem. Soc.* **2006**, *128*, 9026–9027.

(13) Marra, K. G.; Winger, T. M.; Hanson, S. R.; Chaikof, E. L. Cytomimetic Biomaterials. 1. *In-Situ* Polymerization of Phospholipids on an Alkylated Surface. *Macromolecules* **1997**, *30*, 6483–6488.

(14) Mornet, S.; Lambert, O.; Duguet, E.; Brisson, A. The Formation of Supported Lipid Bilayers on Silica Nanoparticles Revealed by Cryoelectron Microscopy. *Nano Lett.* **2005**, *5*, 281–285.

(15) Kallury, K. M. R.; Lee, W. E.; Thompson, M. Enhancement of the Thermal and Storage Stability of Urease by Covalent Attachment to Phospholipid-Bound Silica. *Anal. Chem.* **1992**, *64*, 1062–1068.

(16) Brown, H. A.; Murphy, R. C. Working towards an Exegesis for Lipids in Biology *Nat. Chem. Biol.*, **2009**, *5*, 602–606.

(17) Hsiue, G.-H.; Lee, S.-D.; Chang, P. C.-T.; Kao, C.-Y. Surface Characterization and Biological Properties Study of Silicone Rubber Membrane Grafted with Phospholipid As Biomaterial via Plasma Induced Graft Copolymerization. *J. Biomed. Mater. Res.* **1998**, *42*, 134–147.

(18) Korematsu, A.; Takemoto, Y.; Nakaya, T.; Inoue, H. Synthesis, Characterization and Platelet Adhesion of Segmented Polyurethanes Grafted Phospholipid Analogous Vinyl Monomer on Surface. *Biomaterials* **2002**, *23*, 263–271.

(19) Edinger, K.; Goelzhaeuser, A.; Demota, K.; Woell, C.; Grunze, M. Formation of Self-Assembled Monolayers of n-Alkanethiols on Gold: a Scanning Tunneling Microscopy Study on the Modification of Substrate Morphology. *Langmuir* **1993**, *9*, 4–8.

(20) Meuse, C. W.; Niaura, G.; Lewis, M. L.; Plant, A. L. Assessing the Molecular Structure of Alkanethiol Monolayers in Hybrid Bilayer Membranes with Vibrational Spectroscopies. *Langmuir* **1998**, *14*, 1604–1611.

(21) Terrettaz, S.; Stora, T.; Duschl, C.; Vogel, H. Protein Binding to Supported Lipid Membranes: Investigation of the Cholera Toxin-Ganglioside Interaction by Simultaneous Impedance Spectroscopy and Surface Plasmon Resonance. *Langmuir* **1993**, *9*, 1361–1369.

(22) Lingler, S.; Rubinstein, I.; Knoll, W.; Offenhäusser, A. Fusion of Small Unilamellar Lipid Vesicles to Alkanethiol and Thiolipid Self-Assembled Monolayers on Gold. *Langmuir* **1997**, *13*, 7085–7091.

(23) Wagner, M. L.; Tamm, L. K. Tethered Polymer-Supported Planar Lipid Bilayers for Reconstitution of Integral Membrane Proteins: Silane-Polyethyleneglycol-Lipid as a Cushion and Covalent Linker. *Biophys. J.* **2000**, *79*, 1400–1414.

(24) Atanasov, V.; Knorr, N.; Duran, R. S.; Ingebrandt, S.; Offenhäusser, A.; Knoll, W.; Köper, I. Membrane on a Chip: A Functional Tethered Lipid Bilayer Membrane on Silicon Oxide Surfaces. *Biophys. J.* **2005**, *89*, 1780–1788.

(25) Omae, I. General Aspects of Tin-Free Antifouling Paints. *Chem. Rev.* **2003**, *103*, 3431–3448.

(26) Tria, M. C. R.; Grande, C. D. T.; Ponnapati, R. R.; Advincula, R. C. Electrochemical Deposition and Surface-Initiated RAFT Polymerization: Protein and Cell-Resistant PPEGMEMA Polymer Brushes. *Biomacromolecules* **2010**, *11*, 3422–3431.

(27) Prime, K. L.; Whitesides, G. M. Self-Assembled Organic Monolayers: Model Systems for Studying Adsorption of Proteins at Surfaces. *Science* **1991**, *252*, 1164–1167.

(28) Dalsin, J. L.; Hu, B.-H.; Lee, B. P.; Messersmith, P. B. Mussel Adhesive Protein Mimetic Polymers for the Preparation of Nonfouling Surfaces. *J. Am. Chem. Soc.* **2003**, *125*, 4253–4258.

(29) Christman, K. L.; Schopf, E.; Broyer, R. M.; Li, R. C.; Chen, Y.; Maynard, H. D. Positioning Multiple Proteins at the Nanoscale with Electron Beam Cross-Linked Functional Polymers. *J. Am. Chem. Soc.* **2009**, *131*, 521–527.

(30) Huber, D. L.; Manginell, R. P.; Samara, M. A.; Kim, B.-I.; Bunker, B. C. Programmed Adsorption and Release of Proteins in a Microfluidic Device. *Science* **2003**, *301*, 352–354.

(31) Luk, Y.-FY.; Kato, M.; Mrksich, M. Self-Assembled Monolayers of Alkanethiolates Presenting Mannitol Groups Are Inert to Protein Adsorption and Cell Attachment. *Langmuir* **2000**, *16*, 9604–9608.

(32) Ostuni, E.; Chapman, R. G.; Liang, M. N.; Meluleni, G.; Pier, G.; Ingber, D. R.; Whitesides, G. M. Self-Assembled Monolayers That Resist the Adsorption of

Proteins and the Adhesion of Bacterial and Mammalian Cells. *Langmuir* **2001**, *17*, 6336–6343.

(33) Kane, R. S.; Deschatelets, P.; Whitesides, G. M. Kosmotropes Form the Basis of Protein-Resistant Surfaces. *Langmuir* **2003**, *19*, 2388–2391.

(34) Groll, J.; Amirgoulova, E. V.; Ameringer, T.; Heyes, C. D.; Röcker, C.; Nienhaus, G. U.; Möller, M. Biofunctionalized, Ultrathin Coatings of Cross-Linked Star-Shaped Poly(ethylene oxide) Allow Reversible Folding of Immobilized Proteins. *J. Am. Chem. Soc.* **2004**, *126*, 4234–4239.

(35) Zhang, F.; Kang, E. T.; Neoh, K. G.; Wang, P.; Tan, K. L. Modification of Si(100) Surface by the Grafting of Poly(ethylene glycol) for Reduction in Protein Adsorption and Platelet Adhesion. *J. Biomed. Mater. Res.* **2001**, *56*, 324–332.

(36) Kingshott, P.; Thissen, H.; Griesser, H. J. Effects of Cloud-Point Grafting, Chain Length, and Density of PEG Layers on Competitive Adsorption of Ocular Proteins. *Biomaterials* **2002**, *23*, 2043–2056.

(37) Zhang, Z.; Menges, B.; Timmons, R. B.; Knoll, W.; Förch, R. Surface Plasmon Resonance Studies of Protein Binding on Plasma Polymerized Di(ethylene glycol) Monovinyl Ether Films. *Langmuir* **2003**, *19*, 4765–4770.

(38) Shen, M.; Wagner, M. S.; Castner, D. G.; Ratner, B. D.; Horbett, T. A. Multivariate Surface Analysis of Plasma-Deposited Tetraglyme for Reduction of Protein Adsorption and Monocyte Adhesion. *Langmuir* **2003**, *19*, 1692–1699.

(39) Teare, D. O. H.; Schofield, W. C. E.; Garrod, R. P.; Badyal, J. P. S. Poly(N-acryloylsarcosine methyl ester) Protein-Resistant Surfaces. *J. Phys. Chem. B* **2005**, *109*, 20923–20928.

(40) Chapman, R. G.; Ostuni, E.; Liang, M. N.; Meluleni, G.; Kim, E.; Yan, L.; Pier, G.; Warren, H. S.; Whitesides, G. M. Polymeric Thin Films That Resist the Adsorption of Proteins and the Adhesion of Bacteria. *Langmuir* **2001**, *17*, 1225–1233.

(41) Lasseter, T. L.; Clare, B. H.; Abbott, N. L.; Hamers, R. J. Covalently Modified Silicon and Diamond Surfaces: Resistance to Nonspecific Protein Adsorption and Optimization for Biosensing. *J. Am. Chem. Soc.* **2004**, *126*, 10220–10221.

(42) Teare, D. O. H.; Barwick, D. C.; Schofield, W. C. E.; Garrod, R. P.; Ward, L. J. Badyal, J. P. S. Substrate-Independent Approach for Polymer Brush Growth by

Surface Atom Transfer Radical Polymerization. *Langmuir* **2005**, *21*, 11425–11430.

(43) Bain, C. D.; Troughton, E. B.; Tao, Y. T.; Evall, J.; Whitesides, G. M.; Nuzzo, R. G. Formation of Monolayer Films by the Spontaneous Assembly of Organic Thiols from Solution onto Gold. *J. Am. Chem. Soc.* **1989**, *111*, 321–335.

(44) Stapleton, J. J.; Daniel, T. A.; Uppili, S.; Cabarcos, O. M.; Naciri, J.; Shashidhar, R.; Allara, D. L. Self-Assembly, Characterization, and Chemical Stability of Isocyanide-Bound Molecular Wire Monolayers on Gold and Palladium Surfaces. *Langmuir* **2005**, *21*, 11061–11070.

(45) Ulman, A. Formation and Structure of Self-Assembled Monolayers. *Chem. Rev.* **1996**, *96*, 1533–1554.

(46) Lee, M.-T.; Hsueh, C.-C.; Freund, M. S.; Ferguson, G. S. Air Oxidation of Self-Assembled Monolayers on Polycrystalline Gold: The Role of the Gold Substrate. *Langmuir* **1998**, *14*, 6419–6423.

(47) Yasuda, H. *Plasma Polymerization;* Academic Press: Orlando, 1985.

(48) Ryan, M. E.; Hynes, A. M.; Badyal, J. P. S. Pulsed Plasma Polymerization of Maleic Anhydride. *Chem. Mater.* **1996**, *8*, 37–42.

(49) Friedrich, J. Mechanisms of Plasma Polymerization—Reviewed from a Chemical Point of View. *Plasma Processes Polym.* **2011**, *8*, 783–802.

(50) Ward, L. J.; Schofield, W. C. E.; Badyal, J. P. S.; Goodwin, A. J.; Merlin, P. J. Atmospheric Pressure Glow Discharge Deposition of Polysiloxane and SiOx Films. *Langmuir* **2003**, *19*, 2110–2114.

(51) Ward, L. J.; Schofield, W. C. E.; Badyal, J. P. S.; Goodwin, A. J.; Merlin, P. J. Atmospheric Pressure Plasma Deposition of Structurally Well-Defined Polyacrylic Acid Films. *Chem. Mater.* **2003**, *15*, 1466–1469.

(52) Wood, T. J.; Badyal, J. P. S. Atomized Spray Plasma Deposition (ASPD) of Structurally Well-Defined Alkyl Functionalized Layers. *Surf. Coat. Technol.* **2013**, *227*, 28–31.

(53) Friedman, R. M.; Hudis, J.; Perlman, M. L. Chemical Effects on Linewidths Observed in Photoelectron Spectroscopy. *Phys. Rev. Lett.* **1972**, *29*, 692–695.

(54) Evans, J. F.; Gibson, J. H.; Moulder, J. F.; Hammond, J. S.; Goretzki, H. Angle Resolved ESCA Analysis of Plasma Modified Polysterene *Fresenius J. Anal. Chem.* **1984**, *319*, 841–844.

(55) Lovering, D. *NKD-6000 Technical Manual;* Aquila Instruments: Cambridge, U.K., 1998.

(56) Lin-Vien, D.; Colthup, N. B.; Fateley, W. G.; Grasselli, J. G. *The Handbook of Infrared and Raman Characteristic Frequencies of Organic Molecules;* Academic Press: London, U.K., 1991.

(57) Okouchi, M.; Yamaji, Y.; Yamauchi, K. Contact Angle of Poly(alkyl methacrylate)s and Effects of the Alkyl Group. *Macromolecules* **2006**, *39*, 1156–1159.

(58) Lau, K. K. S.; Gleason, K. K. Initiated Chemical Vapor Deposition (iCVD) of Poly(alkyl acrylates): An Experimental Study. *Macromolecules* **2006**, *39*, 3688–3694.

(59) Harris, L. G.; Schofield, W. C. E.; Doores, K. J.; Davis, B. G.; Badyal, J. P. S. Rewritable Glycochips. *J. Am. Chem. Soc.* **2009**, *131*, 7755–7761.

(60) Ultrasonic-nozzle Product Information, Sono-tek, U.S.A., 1996.

(61) Kolluri, O. S. Ultrasonic Nozzle Feed for Plasma Deposited Film Networks. *PCT International Patent No.* WO 98/10116, 1998.

(62) Altmann, K.; Schulze, R.-D.; Hidde, G.; Friedrich, J. Electrospray Ionization for Deposition of Ultra-thin Polymer Layers – Principle, Electrophoretic Effect and Applications. *J. Adhes. Sci. Technol.* **2013**, *27*, 988–1005.